

# The homing of human cord blood stem cells to sites of inflammation

## Unfolding mysteries of a novel therapeutic paradigm for glioblastoma multiforme

Kiran Kumar Velpula,<sup>1</sup> Venkata Ramesh Dasari<sup>1</sup> and Jasti S. Rao<sup>1,2,\*</sup>

<sup>1</sup>Department of Cancer Biology and Pharmacology; University of Illinois College of Medicine at Peoria; Peoria, IL USA; <sup>2</sup>Department of Neurosurgery; University of Illinois College of Medicine at Peoria; Peoria, IL USA

**Keywords:** IL-8, CXCR-4, CD-8, GRO- $\alpha$ , SDF-1, cord blood stem cells, glioma stem cells

**Abbreviations:** hUCBSC, human umbilical cord blood stem cells; GBM, glioblastoma multiforme; IL-8, interleukin 8; SDF-1, stromal cell derived factor-1; CXCR-4, chemokine receptor 4; GSC, glioma stem cells; CD-8, cluster of differentiation 8

Efficient homing of human umbilical cord blood mesenchymal stem cells (hUCBSC) to inflammation sites is crucial for therapeutic use. In glioblastoma multiforme, soluble factors released by the tumor facilitate the migratory capacity of mesenchymal stem cells toward glioma cells. These factors include chemokines and growth inducers. Nonetheless, the mechanistic details of these factors involved in hUCBSC homing have not been clearly delineated. The present study is aimed to deduce specific factors involved in hUCBSC homing by utilizing a glioma stem cell-induced inflammatory lesion model in the mouse brain. Our results show that hUCBSC do not form tumors in athymic nude mice brains and do not elicit immune responses in immunocompetent SKH1 mice. Further, hUCBSC spheroids migrate and invade glioma spheroids, while no effect was observed on rat fetal brain aggregates. Several cytokines, including GRO, MCP-1, IL-8, IL-3, IL-10, Osteopontin and TGF $\beta$ 2, were constitutively secreted in the naive hUCBSC-conditioned medium, while significant increases of IL-8, GRO, GRO- $\alpha$ , MCP-1 and MCP-2 were observed in glioma stem cell-challenged hUCBSC culture filtrates. Furthermore, hUCBSC showed a stronger migration capacity toward glioma stem cells *in vitro* and exhibited enhanced migration to glioma stem cells in an intracranial human malignant glioma xenograft model. Our results indicate that multiple cytokines are involved in recruitment of hUCBSC toward glioma stem cells, and that hUCBSC are a potential candidate for glioma therapy.

### Introduction

Glioblastoma multiforme (GBM) is a tumor that arises from glia or their precursors within the central nervous system. Currently, no optimal treatment for glioblastoma exists, and patients typically survive less than one year after diagnosis.<sup>1,2</sup> Despite surgical excision and adjuvant radiotherapy and chemotherapy, GBM remains incurable and difficult to treat.<sup>3</sup> This resistance is primarily due to the complex character of the tumor itself, and the inability to deliver therapeutic agents to the tumor.<sup>4</sup> Emerging evidence suggests that glioma stem cells (GSC) are resistant to radiation and chemotherapy and ultimately responsible for the inevitable recurrence and high infiltration of glioblastoma.<sup>5,6</sup> In particular, GSC migration and subsequent invasion of normal neural tissues reduces the effectiveness of delivered therapeutic agents. Thus, clear attempts to deliver therapeutic agents to infiltrate gliomas are necessary to improve brain tumor therapy.

Current efforts involve the use of stem cells in repairing and replacing damaged tissue in order to facilitate functional recovery. Recent evidence suggests that mesenchymal stem cells isolated from bone marrow exhibit tropism for brain tumors and can be used as delivery vehicles.<sup>7</sup> Moreover, locally injected neural stem cells engineered to deliver interleukin-12 reduced the growth of brain tumors.<sup>8,9</sup> Studies suggest that bone marrow-derived mesenchymal stem cells and human cord blood stem cells exhibit high similarity in cell characteristics and multi-lineage differentiation potential.<sup>10-12</sup> Moreover, higher availability and lower immunogenicity of hUCBSC compared with other sources of bone marrow stem cells have made them a considerable resource for cell therapy. However, before the potential of stem cell-based therapies can be realized, the behavior of these cells after implantation *in vivo* and the practicalities of different administration routes must be understood.

Additionally, we and other researchers have previously shown that hUCBSC exhibit extensive migratory capacity and tropism

\*Correspondence to: Jasti S. Rao; Email: jsrao@uic.edu  
Submitted: 03/19/12; Revised: 05/11/12; Accepted: 05/15/12  
<http://dx.doi.org/10.4161/cc.20766>

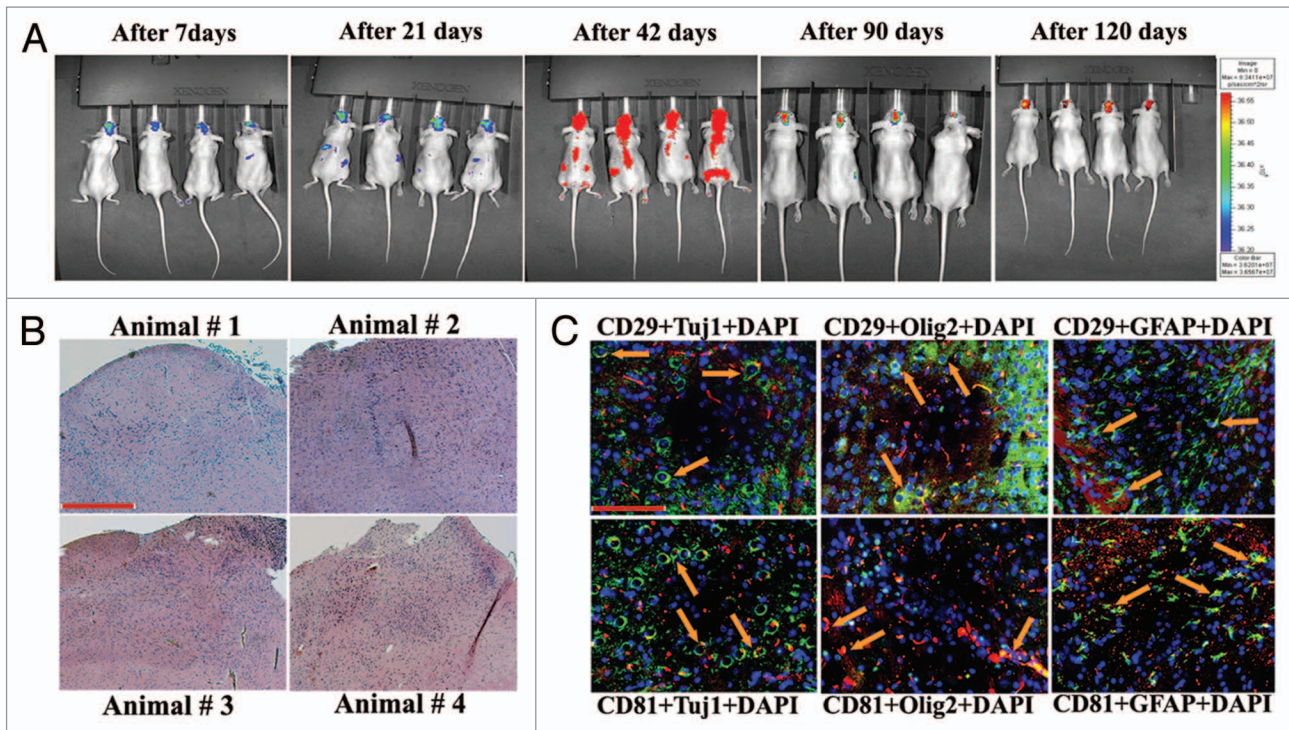


**Figure 1.** In vivo imaging of hUCBSC in nude mice brains. Control hUCBSC ( $0.5 \times 10^6$  cells) stained with Qtracker-Red were injected into the left side of the brain by intracranial implantation and their migration throughout the body of the mice was visualized by in vivo imaging weekly for 120 d using Xenogen IVIS-200 Optical In Vivo Imaging System. (B) hUCBSC-treated nude mice brain sections were stained with Hematoxylin and Eosin to check for tumor growth in nude mice brains. (C) hUCBSC-treated nude mice brain sections were labeled with CD29 and CD81 markers (specific for hUCBSC), Tuj1 (specific for neurons), Olig2 (specific for oligodendrocytes) and GFAP (specific for astrocytes). Co-localization of hUCBSC markers with Tuj1, Olig2 or GFAP indicates that these hUCBSC differentiated into neural cells in the brains of the nude mice. CD29 and CD81 were conjugated with Alexa Fluor 488 secondary antibodies, and Tuj1, Olig2 and GFAP were conjugated with Alexa Fluor 594 secondary antibodies. Bar = 100  $\mu$ m;  $n \geq 4$ .

for gliomas.<sup>13-15</sup> Chemoattractants, namely cytokines and growth factors, likely mediate this migration. The inflamed tumor cells secrete cytokines, such as SDF-1, IL-8, GRO- $\alpha$ , while the cord blood stem cells express receptors such as CXCR4 and CD9. It can be thus hypothesized that interactions between ligands and receptors direct the migration of hUCBSC toward the inflamed cells.<sup>14-17</sup>

We have previously demonstrated that co-culture of hUCBSC with parental glioma cells or glioma stem cells (GSC) significantly inhibits pre-established tumor growth.<sup>13,18-21</sup> Here, we explore how hUCBSC migrate to GSC tumors and regress tumor growth when administered in mice via the tail vein. Our study assesses the expression levels of multiple inflammatory cytokines during hUCBSC migration toward inflammation sites. In addition, we attempt to show the mechanistic role and specificity of hUCBSC in regulating the glioma cell invasion. We also examine the therapeutic role of hUCBSC by using in vitro and in vivo functional assays of migration and homing. Finally, we demonstrate the immunogenicity of hUCBSC when injected intracranially into the immunocompetent mice.

## Results

**hUCBSC did not form tumors in the brains of athymic nude mice.** To confirm whether hUCBSC form tumors in the brains

of athymic nude mice, we injected  $0.5 \times 10^6$  hUCBSC labeled with Qtracker-Red (Invitrogen) into the left side of the brain. Between 14 and 56 d, the stem cells were distributed throughout the entire body (data not shown). After 56 d and up to 90 d, all the stem cells were concentrated only in the brain region. The multiplication and proliferation of hUCBSC in the nude mice brains reached its peak by 90 d, as indicated by red signals when observed using an in vivo Xenogen live imager (Fig. 1A). Observations persisted until 120 d, upon which the intensity of the red signal decreased. The mice were observed to be healthy without any disease symptoms. Our results are in accordance with previous results reported by Devine, et al. (2003);<sup>22</sup> however, the distribution of these stem cells throughout the body needs to be further studied. After 120 d, the mice were euthanized; at that point, the mice appeared healthy and did not exhibit any disease symptoms (data not shown). The brains were formalin fixed for further processing. H&E staining of these nude mice brain sections did not show any tumor formation (Fig. 1B). Brain sections were then analyzed using immunofluorescence with CD29 and CD81 markers (specific for hUCBSC), Tuj1 (specific for neurons), Olig2 (specific for oligodendrocytes) and GFAP (specific for astrocytes). Co-localization of hUCBSC markers with Tuj1, Olig2 or GFAP indicated that these hUCBSC were differentiated to neural cells in the brains of the nude mice (Fig. 1C). These results indicate that hUCBSC in the normal nude mice brains



do not form tumors. Moreover, hUCBSC did differentiate to neural cell types of the host system.

hUCBSC did not elicit an immune response in immunocompetent mice. hUCBSC suppress the allogeneic response of lymphocytes, suggesting its use in allogeneic cell therapies.<sup>23</sup> Several investigators have demonstrated that hUCBSC induces low immunogenicity.<sup>23-27</sup> In the present study, we injected naïve hUCBSC ( $1 \times 10^5$ ) into the brains of euthymic, immunocompetent SKH1 mice (Charles River) via intracranial administration. Separately, human astrocytes ( $1 \times 10^5$ ) were intracranially administered into the brains of SKH1 mice and used as controls. Both hUCBSC and astrocytes were labeled with Cell Tracker-Red CMTPX (Invitrogen) and observed over a period of 4 weeks by in vivo imaging using IVIS200 (Caliper Life Sciences). hUCBSC were distributed throughout the mice as observed by yellow-colored intensity of epifluorescence (Fig. 2A). Presence of cyclosporine showed little effect in the animals treated with hUCBSC. Further, cyclosporine offered little difference in human astrocyte distribution, which was detected until the third week (data not shown). However, no astrocytes were found by the end of the fourth week. Mice were then euthanized and checked for tumor formation in all treatments using H&E staining (Fig. 2B). Infiltration of macrophages was examined by intracranial administration of hUCBSC or astrocytes. Immunostaining of the brain sections by IBA1 antibody revealed that macrophages were abundant in mice injected with astrocytes (without cyclosporine) (Fig. 2C). This finding confirms that hUCBSC neither induced the infiltration of macrophages nor elicited any immune response. Further, we estimated the percentage of CD8<sup>+</sup> cells in all of the animal groups tested. Blood was drawn from the individual mice separately. White blood cells were isolated, labeled with anti-CD8<sup>+</sup> antibody and processed for FACS analysis. hUCBSC did not elicit immune response in both treatments (with or without cyclosporine), as evidenced by the lower percentage of CD8<sup>+</sup> cells compared with control SKH1 mice (Fig. 2D). CD8<sup>+</sup> percentage increased drastically in mice injected with astrocytes, whereas mice injected with astrocytes treated with cyclosporine demonstrated reduced CD8<sup>+</sup> percentage (Fig. 2E). Taken together, our results confirm that hUCBSC do not elicit any immune response in euthymic, immunocompetent mice.

**Inhibitory and chemotactic effects of hUCBSC on glioma migration and invasion.** Previously, we demonstrated that hUCBSC inhibit U251 and 5310 glioma parent cell invasion,

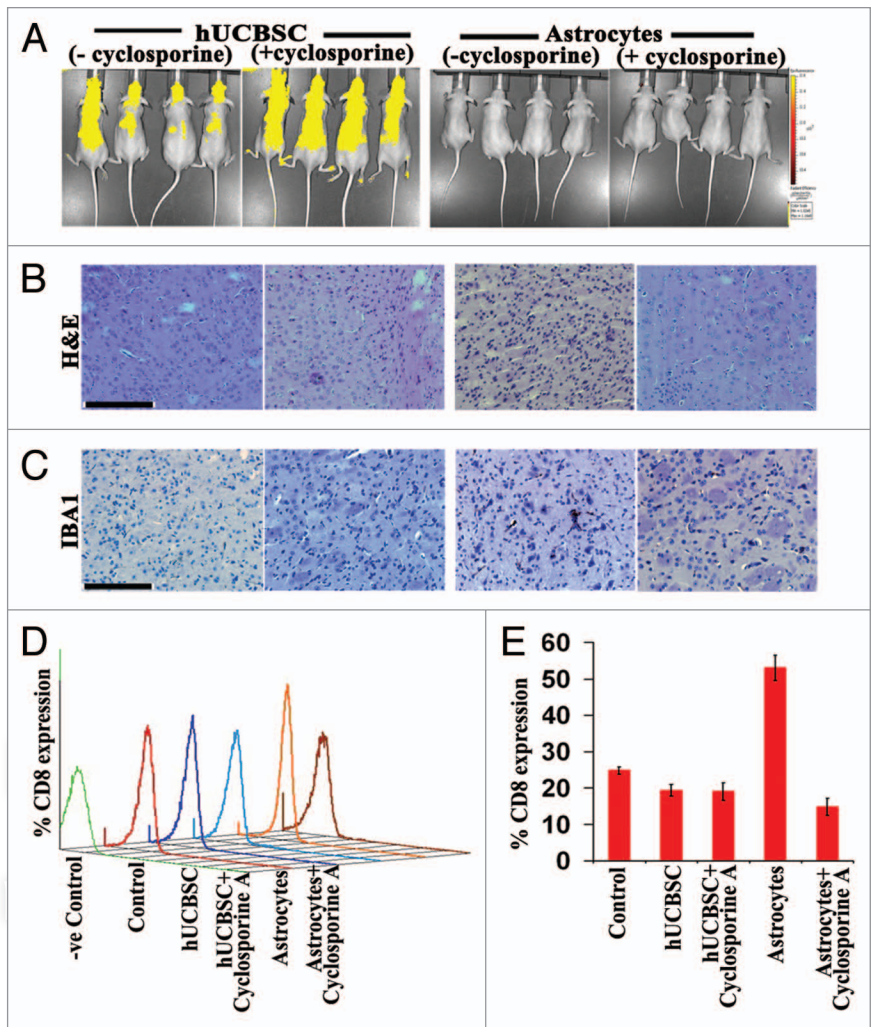


**Figure 2.** Immunogenicity of hUCBSC and human astrocytes in immunocompetent mice. (A) hUCBSC and human astrocytes (250,000 cells each) were injected into the brains of SKH1 mice by intracranial administration. For the cyclosporine group, mice received Cyclosporine-A one day before the injection of cells and at 1 week (10 mg/kg body weight) after the injection of cells. The mice were observed for a period of 4 weeks and then euthanized (n = 6 per group). (B) The brain sections were checked for the presence of tumors by H&E staining. (C) IBA1 staining of the mice by DAB immunohistochemistry. For (B and C), bar = 200  $\mu$ m; n = 4. (D) CD8 cells were isolated from the blood of control and treated mice, labeled with PE-conjugated CD8 antibody, and sorted by FACS analysis; n = 4. (E) Bar diagram representing the percent CD8 expression as depicted by FACS analysis.

migration and progression.<sup>20,28,29</sup> To further investigate the extent of hUCBSC migratory and invasive potential toward glioma cells at the cellular level, we conducted a spheroid invasion assay. The hUCBSC spheroids were labeled with fluorescent CellTracker™ Red, and the glioma spheroids were labeled with fluorescent CellTracker™ Green dye. hUCBSC migrated and engulfed 5310 glioma spheroids by 50% on day 2 and 90% on the day 3, as indicated by yellow-colored merger, (Fig. 3A). To demonstrate glioma cell invasion, glioma cells were confronted against spheroids obtained from the 18-day-old rat fetal brain aggregates labeled with CellTracker™ Red dye. By 72 h, 95% of the glioma spheroids engulfed rat fetal brain aggregates and formed a single entity (Fig. 3B). However, hUCBSC spheroids remained separate

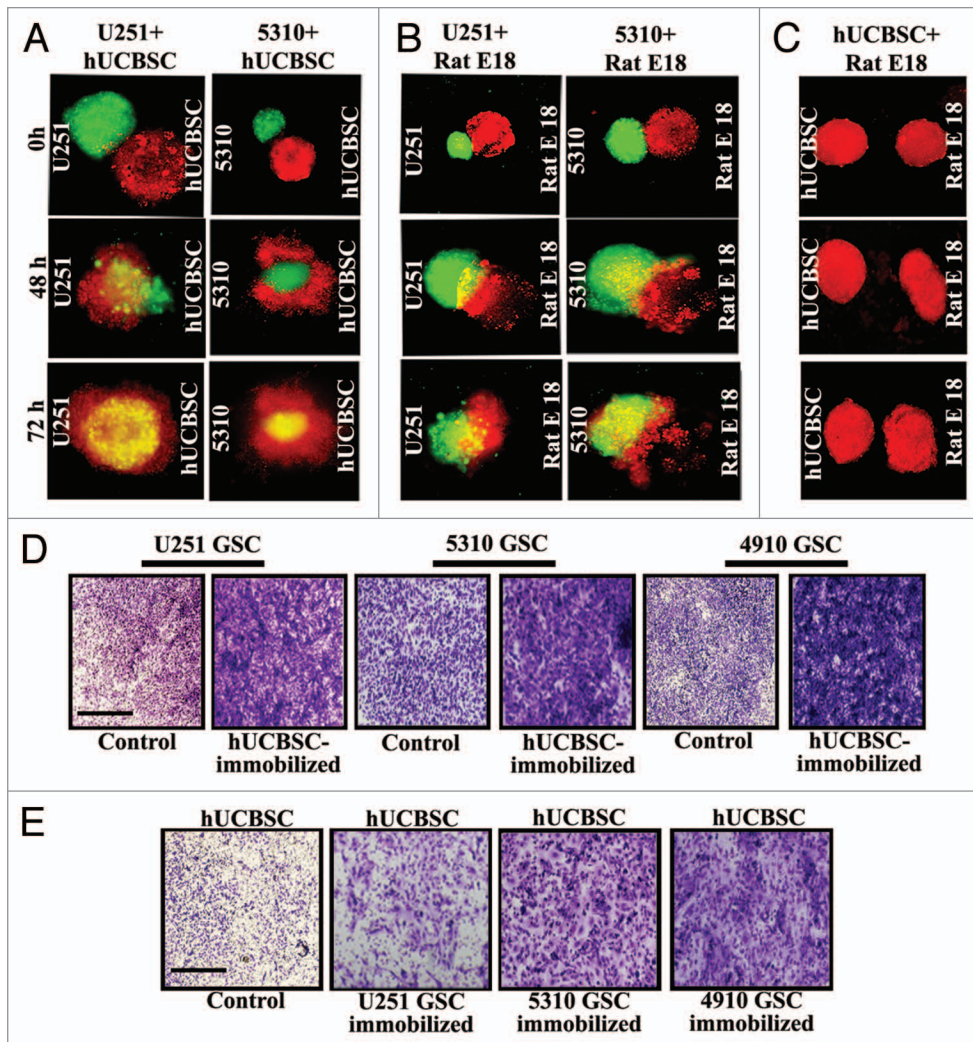


**Figure 3.** Cord blood stem cells inhibit glioma cell migration and invasion. U251 and 5310 glioma spheroids labeled with fluorescent Cell Tracker™ green dye were confronted with hUCBSC and fetal rat brain aggregates labeled with fluorescent CellTracker™ red dye. Progressive destruction of glioma spheroids by hUCBSC spheroids (A) and fetal brain aggregates by glioma tumor spheroids (B) were observed. hUCBSC spheroids remained away from fetal brain aggregates (C) when confronted for 72 h. (D) U251, 5310 and 4910 GSC were allowed to invade through the Matrigel for 24 h. (E) In another experiment, either hUCBSC or glioma cells were immobilized or their counterparts were allowed to pass through the Matrigel. After 24 h, migrated cells in all of the treatments were counted under the microscope.

from 18-day-old rat fetal brain aggregates (Fig. 3C), suggesting hUCBSC specificity toward the pathogenic condition. Upon observing hUCBSC migration toward glioma spheroids and to explore the chemotactic effect of hUCBSC in regulating glioma stem cell invasion and migration, we immobilized and supplemented hUCBSC with complete medium using the Matrigel Transwell system. U251, 5310 and 4910 GSC were cultured in the upper chamber. After culturing, glioma stem cells migrated more effectively toward the hUCBSC, thereby suggesting its chemoattractive behavior (Fig. 3D). In another experiment, U251, 5310 and 4910 glioma stem cells were immobilized, and hUCBSC were cultured in the Matrigel chamber. hUCBSC did migrate to the lower chamber but in relatively fewer numbers (Fig. 3E). These data suggest the existence of certain soluble factors that

hUCBSC might be possibly secreting into the surrounding medium to facilitate chemotactic movement toward malignant cells.

**Inflammation mediates hUCBSC migration.** Several researchers have demonstrated the expression of hUCBSC secretory soluble factors into the surrounding medium.<sup>14,30,31</sup> Based on our previous studies, we propose that the hUCBSC demonstrate conditional behavior toward glioma cells. To test our hypothesis, we studied the cytokine profile from hUCBSC-conditioned medium using a cytokine antibody array. We observed the constitutive secretion of numerous chemokines, including GRO, MCP-1, IL-8, IL-3, IL-10, Osteopontin, NAP-2, IGFBP-2, TIMP2, MDC, Rantes and TGFβ2, in the naive hUCBSC-conditioned medium (Fig. 4A). To determine if hUCBSC secrete other soluble factors exposed to malignant glioma cells, we immobilized hUCBSC under serum-free medium in the lower Boyden chamber. In the upper compartment, we cultured highly invasive 4910 glioma stem cells. The chamber was incubated for 24 h. hUCBSC culture filtrates were then subjected for cytokine array analysis. We observed significant increases of IL-8, GRO, GRO-α, MCP-1 and MCP-2, along with IL-6 expression, when compared with the protein studies in the nascent hUCBSC-conditioned medium (Fig. 4B). Interestingly, the expres-

sion levels of Osteopontin, MDC, RANTES, IL-3 and IL-10 were decreased in the hUCBSC-challenged culture filtrates, while oncostatin and VEGF newly appeared in the latter array (Fig. 4B). To study the expression profiles of these cytokines in co-culture, we subjected hUCBSC, U251, 5310 and 4910 glioma stem cells along with their respective hUCBSC co-cultured culture filtrates for immunoblot analysis. Western blotting using IL-8, SDF1, MCP-1 and GRO-α demonstrated an increased expression of these cytokines in the hUCBSC co-cultured lysates when compared with their respective control glioma stem cells (Fig. 4C). We then studied the expression of receptors CXCR4 and CD9 in the tissue lysates of hUCBSC, U251, 5310 and 4910 glioma stem cells and their hUCBSC treated counterparts in the mouse xenografts. Negligible expression of both molecules was observed



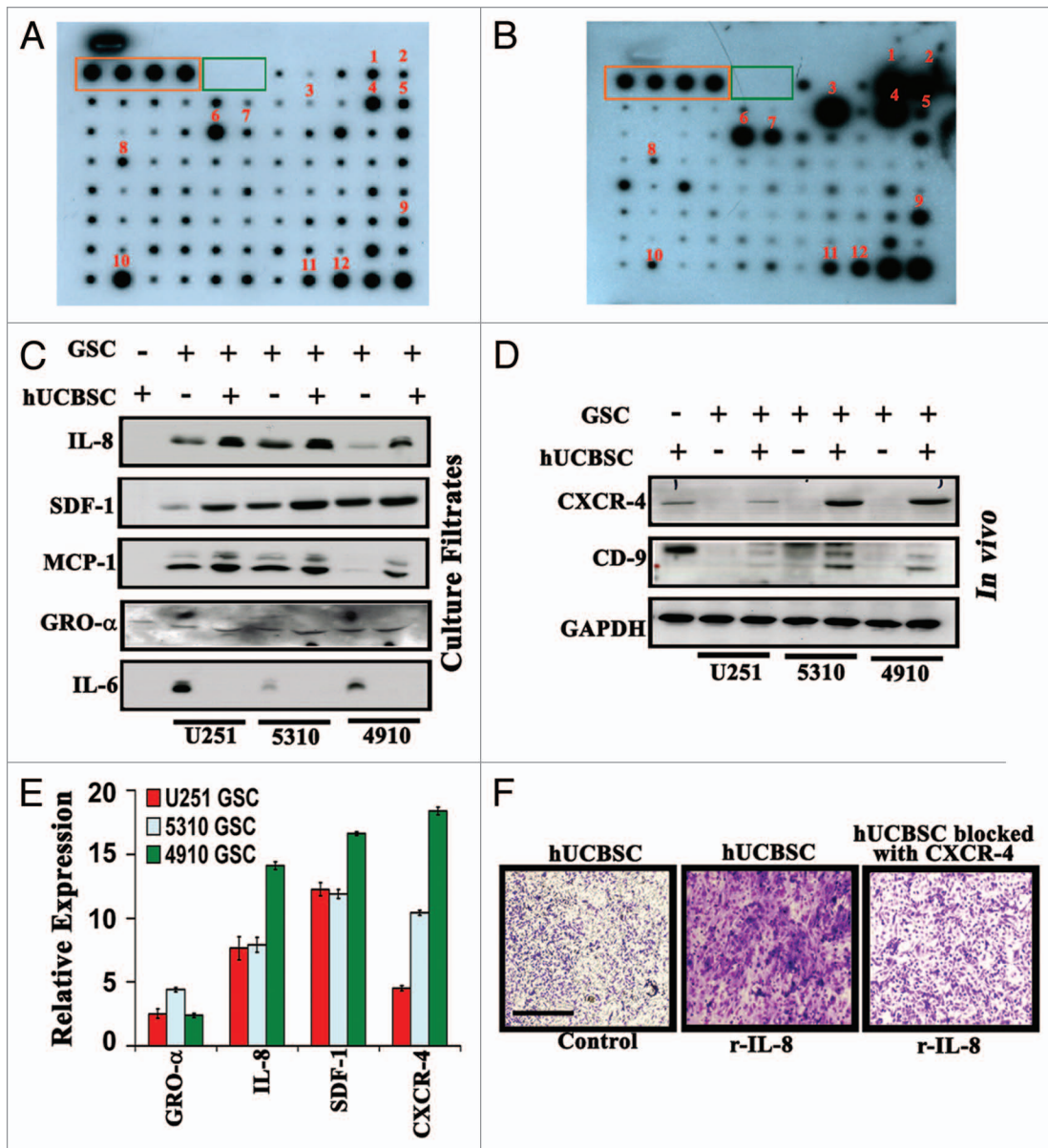


**Figure 4.** Upregulation of various cytokines in culture filtrates of hUCBSC challenged with 4910 GSC. Conditioned media was collected from hUCBSC and hUCBSC challenged with 4910 GSC. The culture filtrates were incubated on the array membrane and visualized by ECL reagents as described in Materials and Methods. The orange and green boxes represent the positive and negative controls, respectively. (A) Cytokine antibody array analysis of hUCBSC. (B) Cytokine antibody array analysis of challenged hUCBSC. (1:GRO; 2:GRO- $\alpha$ ; 3:IL-6; 4:IL-8; 5:IL-10; 6:MCP-1; 7:MCP-2; 8:Rantes; 9:IGFBR2; 10:Osteopontin; 11:TIMP-1; 12:TIMP-2). (C) Levels of IL-8, SDF1, MCP-1, GRO- $\alpha$  and IL-6 were detected by western blotting of culture filtrates of control hUCBSC, GSC and GSC co-cultures with hUCBSC. (D) Total protein was simultaneously isolated from mouse xenografts for western blotting to determine the expression of CXCR4 and CD9. The blots were stripped and reprobbed with GAPDH antibody as a loading control. (E) Measurement of the levels of GRO- $\alpha$ , IL-8, SDF-1 and CXCR4 by RT-PCR in U251, 5310 and 4910 GSCs co-cultured with hUCBSC. Fold changes relative to the control are shown. (F) In vitro migration assay of hUCBSC toward recombinant IL-8. Representative photomicrographs of stained Matrigel demonstrating migration of control hUCBSC and CXCR4 functionally blocked hUCBSC toward the conditioned medium substituted with 10 ng/mL recombinant IL-8. Cell migration was evaluated after staining from randomly selected fields, enumerating migrating cells ( $n = 3$ ).

in controls, while the hUCBSC and hUCBSC-treated sections demonstrated increased expression levels, suggesting the possible interaction of these receptors with the respective growth factors and cytokines (Fig. 4D). RT-PCR conducted with the cDNA of the abovementioned tissues produced similar results to our western blot analysis (Fig. 4E). Additionally, our Boyden chamber results indicated that addition of recombinant IL-8 increases

hUCBSC migration, whereas functional blocking of CXCR4 in the hUCBSC promoted poor migration, even when supplemented with recombinant IL-8 (Fig. 4F). These results suggest that the migration or homing of the hUCBSC might be due to multiple factors regulating their migration toward sites of inflammation.

hUCBSC is home to glioma tumors when injected via the tail vein in nude mice. After establishing the role of hUCBSC

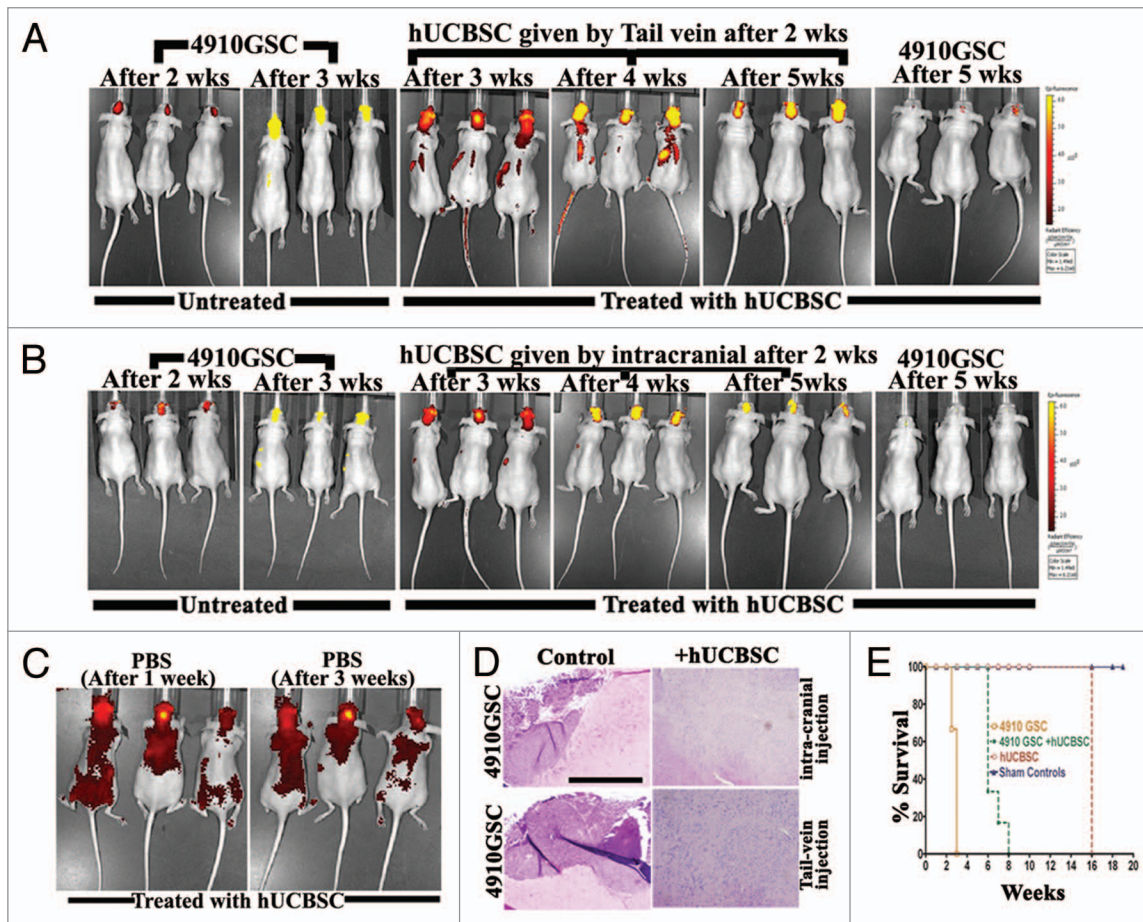


**Figure 5.** Homing of hUCBSC toward tumors in the mice brains. 4910 GSC (250,000 cells) were injected into the brains of athymic nude mice by intracranial administration. After 2 weeks, hUCBSC (250,000 cells) were injected into either (A) the tail vein or (B) intracranially (contra-lateral) and observed for 3 weeks. From the 2<sup>nd</sup> week until the end of the 5<sup>th</sup> week, mice were subjected to in vivo imaging using the IVIS Imaging System (n = 6 for each group). (C) Mice brains were injected with 10  $\mu$ L of sterile PBS by intracranial administration. After 1 week, labeled hUCBSC (250,000 cells) were injected by through the tail vein and observed for homing by in vivo imaging; n = 3. (D) The brain sections of mice (A and B) were checked for the presence of tumor formation by H&E staining; bar = 500  $\mu$ m; n = 3. (E) Survival curves were plotted for control and treated mice.

in migration and immunogenicity, we evaluated their characteristic property of homing toward tumor cells in mice brains. We implanted 4910 GSC (labeled with cyto-tracker green dye) into the athymic nude mice brains via intracranial administration. The aggregated cells (tumors) were observed after 2 weeks and confirmed by in vivo imaging (Fig. 5A). We then administered hUCBSC (labeled with cyto-tracker red dye) via the tail vein or intracranial administration (contra-lateral). The mice were observed for 3 weeks by in vivo imaging to analyze the homing efficiency of hUCBSC toward the tumor cells. Cord blood stem cells injected by the tail vein migrated toward the brain tumors, and by the end of the fifth week, they were concentrated on the tumors of the mice brains (Fig. 5A). We also observed that cord blood stem cells injected contra-laterally also migrated toward the tumor cells (Fig. 5B). In both cases, we observed the regression of the tumors by 70–90% (Fig. 5A, B and D), as evidenced by H&E stain. As a control, we injected sterile PBS into the mice brains, and after one week, the labeled hUCBSC were injected by the tail vein and observed for 3 weeks. As there was no specific trauma or inflammation, the cord blood stem cells migrated and

distributed throughout the body regions (Fig. 5C). These results confirm that hUCBSC migrated toward the regions of stress or inflammation or tumors in the mice body, and their migration was specific to the point of stress or inflammation. Mice injected with 4910 GSC demonstrated glioma characteristics within 2 to 3 weeks. hUCBSC injected into pre-established 4910 GSC tumors increased the lifespan of mice until 8 weeks. Although healthy, animals injected with only hUCBSC were euthanized after 120 d. Sham controls (mice injected with only phosphate buffered saline) were left alone till the completion of the experiment (Fig. 5E).

Multiple factors articulate the homing of hUCBSC toward glioma stem cells. Cytokines, growth factors and their receptors regulate mesenchymal stem cell migration.<sup>32,33</sup> Previous studies, including our own, revealed that neuronal stem cells/cord blood stem cells migrate toward glioma cells mediated by SDF-1 $\alpha$ . SDF-1 $\alpha$  functions as a chemoattractant for hematopoietic cells, facilitating their transmigration through endothelial cell barriers.<sup>13,14,34</sup> Kim et al.,<sup>14</sup> using U87 malignant glioma parent cells, demonstrated that cord blood stem cells exhibit high



migratory capacity toward the malignant U87 parental glioma cells and attributed their chemotactic migration to high levels of IL-8 production. Based on prior literature, we attempted to unravel the migratory/homing potential of cord blood stem cells toward the glioma stem cells. To examine the mechanisms by which hUCBSC home to glioma tissues, we examined the expression levels of cytokine IL-8, factor SDF1 and receptor CXCR4 in control hUCBSC, 4910 GSC and hUCBSC-treated (tail vein) tumor sections. CXCR4 was highly expressed in the control hUCBSC and hUCBSC-treated brains as compared with 4910 GSC control brain sections (Fig. 6A). In another experiment, we studied the expression levels of IL-8 and SDF1 in both control and hUCBSC-treated mice brain tumor sections. IL-8 and SDF1 expression was observed in all tested conditions, while hUCBSC-treated sections demonstrated an increased expression of these molecules when compared with the controls (Fig. 6B and C). All immunohistochemical analysis was performed using CD81 (mesenchymal stem cell marker). Negligible CD81 levels were observed in the control 4910 glioma stem cell sections, whereas hUCBSC and hUCBSC-treated brain sections showed high expression levels of CD81 (Fig. 6A–C). Collectively, these results indicate that hUCBSC might employ multiple factors in homing toward glioma stem cells.

## Discussion

Glioblastoma multiforme is the most common intracranial tumor in adults and is characterized by extensive heterogeneity, both at the cellular and molecular levels. Different tumor cell populations establish a complex network of interactions between each other and within the tumor microenvironment, thereby strengthening tumor growth.<sup>35</sup> Glioblastoma migration and invasion operates primarily due to multiple genetic alterations and signaling pathways. This invasive behavior spreads individual tumor cells into regions of brain essential for survival of the patient, which makes the cancer difficult to target and treat. The complexity of glioma tumors is increased by the discovery of differences in the phenotype of cancer stem cells derived from tumors of equivalent histological class and grade.<sup>36,37</sup>

It has been reported that neural stem cells engineered to deliver tumor necrosis factor-related, apoptosis-inducing ligand inhibits the growth of brain tumors.<sup>8</sup> In the present study, we elucidated the pathogenic-specific mechanism of hUCBSC. From spheroid invasion experiments, hUCBSC migrate and invade the glioma spheroids, indicating their tropism and regulation of glioma infiltration by inducing apoptosis. In this process, hUCBSC also prevent migration upon their encounter with the pathogenic glioblastoma. When confronted with fetal rat brain aggregates, hUCBSC did not migrate. Further, Matrigel experiments conducted using hUCBSC demonstrate the functional ability of the hUCBSC in crossing the blood-brain barrier. We observed that immobilized hUCBSC attract the glioma stem cells, whereas challenged hUCBSC are attracted toward the glioma, suggesting their conditional behavior in treating pathological glioblastoma.

Recent use of mesenchymal stem cells for glioma treatment depends on tumor tropism,<sup>14,15,38,39</sup> it was reported that soluble

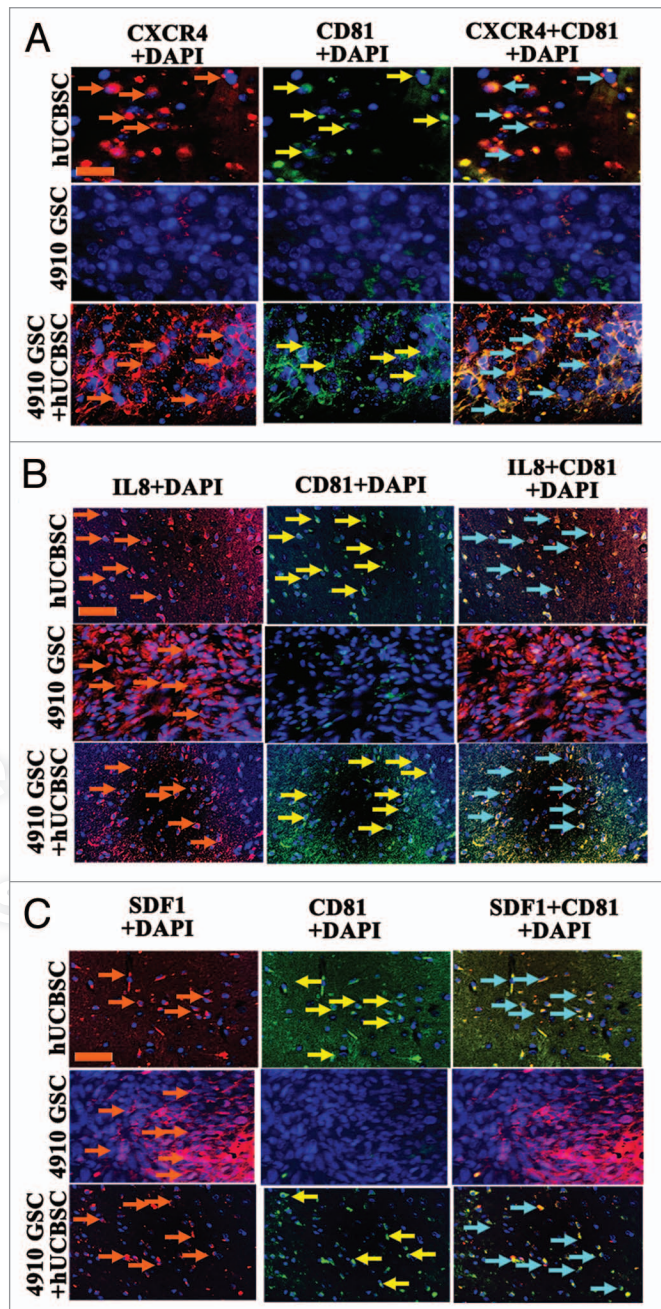


**Figure 6.** Inflammatory cytokines drive hUCBSC migration toward glioma stem cells. Nude mice with pre-established intracranial human glioma stem cell tumors (4910 GSC) were treated via injection of hUCBSC via the tail vein. The hUCBSC-treated and control brain sections were harvested, sectioned and immunoprobed for the presence of CXCR4, IL-8 and SDF1 using appropriate secondary antibodies. Each experiment was performed in duplicate with each sample (n = 6). (A) CXCR4 expression was observed only in hUCBSC and hUCBSC-treated brain samples. Brown colored arrow indicates CXCR4 expression. (B) IL-8 expression was observed in hUCBSC, 4910 GSC control and hUCBSC-treated sections. Brown colored arrow demonstrates IL-8 expression. (C) SDF1 expression was observed more in the 4910 GSC sections as compared with hUCBSC and hUCBSC-treated sections. Brown colored arrow indicates SDF1 expression. The yellow colored arrow indicates CD81 expression, whereas the blue colored arrow represents CD81 co-localization. In all cases, DAPI was used to stain the nuclei; bar = 200  $\mu$ m.

**Table 1.** Primer sequences for the target genes

Gene	Forward primer	Reverse primer
GRO- $\alpha$	5'-AGG GAA TTC ACC CCA AGA AC-3'	5'-TGG ATT TGT CAC TGT TCA GCA-3'
IL-8	5'-TTT TGC CAA GGA GTG CTA AAG A-3'	5'-AAC CCT CTG CAC CCA GTT TTC-3'
SDF-1	5'-CTT CAG ACA CTG AGG CTC CC-3'	5'-AGG CAA TCA CAA ACC CAG TC-3'
CXCR-4	5'-TCA TCT ACA CAG TCA ACC TCT ACA-3'	5'-GAA CAC AAC CAC CCA CAA GTC ATT-3'
$\beta$ -actin	5'-GGC ATC CTC ACC CTG AAG TA-3'	5'-GGG GTG TTG AAG GTC TCA AA-3'

factors secreted from tumors mediate hUCBSC tropism toward glioma cells. Earlier, Schimdt et al.<sup>40</sup> demonstrated that the tropism of neural stem cells is dependent on the overexpression of VEGF by glioma cells along with cytokines like CXCR4 and CXCL12. Kim et al.<sup>41</sup> conducted *in vivo* efficacy experiments and showed that intratumoral injection of engineered hUCBSC significantly inhibited tumor growth and prolonged the survival of glioma-bearing mice as compared with controls. Ryu et al. (2011),<sup>42</sup> recently studied the migratory capacity of hUCBSC mediated by IL-12 toward GL26 mouse glioma cells *in vitro* and *in vivo* in gliomas implanted in C57BL/6 mice. Similarly, Park, et al.<sup>43</sup> found that overexpression of the SDF-1 $\alpha$  receptor CXCR4 in hUCBSC enhanced the migratory capacity toward gliomas. Several researchers have observed that cytokines, such as IL-6, IL-8, MCP-1, Rantes, GRO and GRO- $\alpha$ , were constitutively expressed by both the bone marrow stem cells and umbilical cord blood stem cells.<sup>31</sup> Our results, obtained by challenging hUCBSC with glioma stem cells, are in agreement with the previously published results. Western blot and RT-PCR analyses conducted on the culture filtrates demonstrated increased expression levels of these cytokines along with the homing receptors CXCR4 and CD9 in hUCBSC and hUCBSC co-cultured xenograft lysates.

Various sources of mesenchymal stem cells exist, such as the bone marrow, adipose tissue, umbilical cord blood and placenta. hUCBSC utilization offers significant advantages, which include relative ease of availability, tumor tropism and infiltrative potential across the blood brain barrier. In the present study, we observed that hUCBSC possessed the ability to cross the blood-brain barrier of glioblastoma tumor bearing athymic mice and showed higher seeding efficiency when compared with the mice with no glioblastoma tumors. This observation was similar to the other studies, which demonstrated that mesenchymal stem cells have the capability to cross the blood brain barrier of rats after artificial cerebral ischemia.<sup>44</sup> Later an important role for chemokines (CCL2, CCL3 and CXCL12) involvement in mediating mesenchymal stem cell migration in the ischemic brain was evidently shown.<sup>45,46</sup> Furthermore, Ji et al. (2004) provided an important insight into the understanding of the mechanisms governing the trafficking of transplanted mesenchymal stem cells. These data suggested that the interactions of some chemokines-chemokine receptors, such as fractalkine-CX3CR1 and

SDF-1-CXCR4, could partially mediate the trafficking of these cells to impaired sites in the brain. Moreover, in a previous study, Bieback et al. (2004) demonstrated that transplanted human umbilical cord blood stem cells were used to treat inborn metabolic errors. Additionally, unlike embryonic stem cells, hUCBSC showed low levels of HLA antigens<sup>49</sup> with no evidence of forming teratomas.<sup>50</sup> Further, hUCBSC did not trigger immune reactions, even in unrelated donor transplantation.<sup>51</sup> In the present study, we injected hUCBSC and astrocytes into immunocompetent mice. In another cohort, we administered hUCBSC and astrocytes along with the common immunosuppressant Cyclosporine-A. Mice injected with hUCBSC and hUCBSC treated with Cyclosporine-A demonstrated normal CD8<sup>+</sup> levels as compared with the control mice. The cohort with astrocytes demonstrated a dramatic increase in the CD8<sup>+</sup> expression levels, whereas the cohort of astrocytes treated with Cyclosporine-A behaved normally. Interestingly, graft rejection was not observed in any of these treatments. Our IBA1 staining confirming the absence of teratomas is similar to the previous studies, thus confirming the potential use of hUCBSC for the allogenic treatment of glioma.

Due to their ability to repair damaged or inflamed tissues, hUCBSC offer a potential treatment option in clinical therapy. Although several researchers have shown the possible role of cytokines in regulating the homing of hUCBSC, we demonstrated the possibility of multiple cytokines being secreted from the inflamed glioma tissues, affecting the expression of co-stimulatory receptor molecules and aiding in increased homing of hUCBSC. Our experiments also demonstrated that hUCBSC control the GSCs when encountered. In conclusion, our findings provide detailed analysis of the effects of hUCBSC in homing, migration, invasion and immunogenicity, thereby providing more insights into human stem cell biology.

## Materials and Methods

**Antibodies and reagents.** We used the following antibodies: mouse anti-IL-6, mouse anti-IL-8, goat anti-GRO- $\alpha$ , mouse anti-MCP-1, rabbit anti-SDF-1, rabbit anti-CXCR4, rabbit anti-CD9, rabbit-anti-IBA1 and mouse anti-GAPDH (1:200 dilution). All these antibodies were obtained from Santa Cruz Biotechnology. Recombinant IL-8 was obtained from R and D Systems.

**Preparation and culture of human umbilical cord blood stem cells (hUCBSC).** Human umbilical cord blood samples were collected from the umbilical vein of newborns with informed maternal consent according to the protocol approved by the Institutional Review Board at the University Of Illinois College Of Medicine at Peoria. hUCBSC harvests were processed within 24 h of collection, with viability of more than 90%. Isolation, culture and expansion of hUCBSC were performed as described previously in reference 28.

**Glioma cell cultures.** U251 cells obtained from the National Cancer Institute (NCI) were grown in DMEM supplemented with 10% fetal bovine serum (FBS) (Hyclone) and 1% penicillin-streptomycin (Invitrogen). Xenograft parent cell lines 4910 and 5310 (a kind gift from Dr. David James at University of California)



were grown in RPMI-1640 medium supplemented with 10% FBS and 1% penicillin-streptomycin at 37°C in a humidified atmosphere containing 5% CO<sub>2</sub>. GBM neurospheres of the 4910 xenograft cell line were cultured in neurobasal medium supplemented with N2 (1%), B27 (1%), 20 ng/mL bFGF, 20 ng/mL EGF and 10 ng/mL LIF (Millipore).<sup>52</sup> Experiments for the present study were conducted using the neurospheres of the eighth passage. Human astrocytes were purchased from ScienCell Research Laboratories and grown in astrocyte medium supplemented with 2% FBS, 1% penicillin-streptomycin and 1% astrocyte growth supplements.

**Spheroid invasion assay.** U251, 5310, hUCBSC and fetal rat brain cells (each 1 x 10<sup>6</sup>/mL) were cultured in low-attachment, 48-well culture plates with constant shaking until multicellular spheroids formed. Single glioma spheroids with a diameter of 100–200 μm were placed in the center of each well of a 48-well microplate. In separate experiments, hUCBSC spheroids and fetal rat brain aggregates were confronted with glioma spheroids and each other as well. U251 and 5310 glioma spheroids were labeled with fluorescent CellTracker™ Green CMFDA (5-chloromethylfluorescein diacetate) dye. Both hUCBSC and fetal rat brain aggregates were labeled with fluorescent CellTracker™ Red CMPTX (Invitrogen Molecular Probes). Migration was monitored for 72 h. Progression of U251 and 5310 spheroids was observed under a confocal laser scanning microscope and photographed as described previously in reference 53.

**Migration and chemotaxis assays.** Migration (in vitro) was studied using Transwell migration assays. U251, 5310 and 4910 GSCs (1 x 10<sup>5</sup>) along with CXCR4, SDF-1 and GRO-α were added to the upper compartment while the lower compartment contained immobilized hUCBSC. In another experiment hUCBSC (1 x 10<sup>5</sup>) were added to the upper chamber with the lower chamber containing immobilized U251, 5310 and 4910 GSCs along with recombinant IL-8 (10 ng/mL). Similarly, hUCBSC were subjected to functional blocking using CXCR4 and challenged with recombinant IL-8. In all cases, culture supernatants in the lower chamber were used as chemoattractants. After 24 h, invaded cells were fixed, stained with Hema 3 and counted under a light microscope.

**Cytokine antibody array.** One milliliter of conditioned medium from the hUCBSC control and hUCBSC challenged with 4910 GSC were subjected to human cytokine antibody array (Ray Biotech) to detect the presence of cytokines. The assays were performed as per the manufacturer's instructions.

**Reverse transcription PCR analysis.** Primer sequences were designed from human GenBank sequences using Primer 3 software (v.0.4.0). For real time polymerase chain reaction (RT-PCR) analysis, total cellular RNA was isolated using the RNeasy kit (Qiagen). Total RNA was reverse transcribed into first strand cDNA using the Transcriptor First Strand cDNA Synthesis Kit (Roche). Target primers for the amplification of IL-8, GRO-α, SDF-1 and CXCR4 are listed in Table 1. Reverse transcriptase PCR was conducted using the following PCR cycle: 95°C for 5 min, (95°C for 45 sec, 55–60°C for 45 sec and 72°C for 45 sec) x35 cycles, 72°C for 10 min. Each sample was measured in triplicate and normalized to β-actin gene expression.

**Western blot analysis.** Western blotting was performed as described previously in reference 29. Culture filtrates were collected after 24 h from all of the treatment conditions. Culture filtrates, treated cell lysates and controls were subjected to SDS-PAGE analysis, followed by transfer to nitrocellulose membrane (Bio-Rad). The membranes were then probed with specific primary and secondary antibodies.

**CD8<sup>+</sup> estimation by FACS analysis.** The Institutional Animal Care and Use Committee of the University of Illinois College of Medicine at Peoria approved all surgical interventions and post-operative animal care. Immunocompetent mice SKH-1 were injected intracranially with hUCBSC or human astrocytes. Cyclosporine (10 mg/kg) (Bedford Labs) was administered to another group for one week. A cohort of six animals was used for this study. Whole blood was collected from animals just before complete euthanization. Buffy coat containing white blood cells (WBC) was collected from blood after centrifugation. WBC obtained from various treatment groups were labeled with FITC-conjugated CD8<sup>+</sup> (BD Biosciences). Isotypic negative controls were used to establish background fluorescence. Positive cells were identified after excitation with the appropriate laser. Ten thousand events were counted for each analysis, and all experiments were performed in quadruplicate for each group.

**Immunohistochemical staining.** Tissue sections were de-paraffinized and subjected to antigen retrieval for 10 min at 90°C in 0.1 M sodium citrate buffer (pH 6.0). After permeabilizing with 0.3% Triton X-100, tissue sections were incubated with respective primary antibodies overnight at 4°C. For secondary antibody labeling, HRP-conjugated antibodies were used. These sections were washed in PBS and developed with the diaminobenzidine (DAB) substrate (Sigma-Aldrich) to produce color. After counterstaining with Hematoxylin, sections were mounted, cleared, coverslipped and examined using a confocal microscope. Cell nuclei were counterstained with DAPI (10 ng/mL, Sigma). For immunofluorescence, sections were treated with primary antibodies overnight at 4°C and then treated with appropriate Alexa Fluor secondary antibodies at room temperature for 1 h. Negative controls were maintained either without primary antibody or using IgG. All immunostained sections, which were stained with fluorescent antibodies, were counterstained with DAPI. The sections were blind reviewed by a neuropathologist.

**Intracranial administration of hUCBSC in vivo.** Approximately 250,000 4910 GSC were injected intracerebrally into the right side of nude mice brains under isoflurane anesthesia with the aid of a stereotactic frame. hUCBSC (250,000) labeled with fluorescent CellTracker™ Red CMPTX (Invitrogen Molecular Probes) were injected left of the sagittal suture and bregma of mouse brain two weeks after tumor implantation. The ratio of the hUCBSC to cancer cells was maintained at 1:1. In another experiment, hUCBSC labeled with fluorescent CellTracker™ Red CMPTX (250,000 cells/50 μL) were injected via the tail vein two weeks after tumor implantation. From the second week until the fifth week, the mice were visualized using the IVIS Imaging System. Mice injected with 10 μL of sterile PBS were treated as controls. Paraffin-embedded sections were stained with Hematoxylin and Eosin (H&E) to visualize tumor regression.

**Statistical analysis.** Quantitative data from cell counts, FACS analysis and RT-PCR were evaluated for statistical significance using one-way analysis of variance (ANOVA). Data for each treatment group are represented as mean  $\pm$  SEM and compared with other groups for significance by one-way ANOVA using Graph Pad Prism version 3.02, a statistical software package (NIH).

#### Disclosure of Potential Conflicts of Interest

No potential conflicts of interest were disclosed.

#### References

- Fine HA, Dear KB, Loeffler JS, Black PM, Canellos GP. Meta-analysis of radiation therapy with and without adjuvant chemotherapy for malignant gliomas in adults. *Cancer* 1993; 71:2585-97; PMID:8453582; [http://dx.doi.org/10.1002/1097-0142\(19930415\)71:8<2585::AID-CNCR2820710825>3.0.CO;2-S](http://dx.doi.org/10.1002/1097-0142(19930415)71:8<2585::AID-CNCR2820710825>3.0.CO;2-S).
- Surawicz TS, Davis F, Freels S, Laws ER Jr, Menck HR. Brain tumor survival: results from the National Cancer Data Base. *J Neurooncol* 1998; 40:151-60; PMID:9892097; <http://dx.doi.org/10.1023/A:1006091608586>.
- Aboody KS, Najbauer J, Danks MK. Stem and progenitor cell-mediated tumor selective gene therapy. *Gene Ther* 2008; 15:739-52; PMID:18369324; <http://dx.doi.org/10.1038/gt.2008.41>.
- Louis DN, Posner J, Jacobs T, Kaplan R. Report of the Brain Tumor Progress Review Group. National Institute of Neurological Disorders and Stroke 2000; 1-96.
- Bao S, Wu Q, McLendon RE, Hao Y, Shi Q, Hjelmeland AB, et al. Glioma stem cells promote radioresistance by preferential activation of the DNA damage response. *Nature* 2006; 444:756-60; PMID:17051156; <http://dx.doi.org/10.1038/nature05236>.
- Liu G, Yuan X, Zeng Z, Tunici P, Ng H, Abdulkadir IR, et al. Analysis of gene expression and chemoresistance of CD133<sup>+</sup> cancer stem cells in glioblastoma. *Mol Cancer* 2006; 5:67; PMID:17140455; <http://dx.doi.org/10.1186/1476-4598-5-67>.
- Nakamizo A, Marini F, Amano T, Khan A, Studeny M, Gumin J, et al. Human bone marrow-derived mesenchymal stem cells in the treatment of gliomas. *Cancer Res* 2005; 65:3307-18; PMID:15833864.
- Ehteshami M, Kabos P, Gutierrez MA, Chung NH, Griffith TS, Black KL, et al. Induction of glioblastoma apoptosis using neural stem cell-mediated delivery of tumor necrosis factor-related apoptosis-inducing ligand. *Cancer Res* 2002; 62:7170-4; PMID:12499252.
- Ehteshami M, Kabos P, Kabosova A, Neuman T, Black KL, Yu JS. The use of interleukin 12-secreting neural stem cells for the treatment of intracranial glioma. *Cancer Res* 2002; 62:5657-63; PMID:12384520.
- Kern S, Eichler H, Stoeve J, Klütter H, Bieback K. Comparative analysis of mesenchymal stem cells from bone marrow, umbilical cord blood or adipose tissue. *Stem Cells* 2006; 24:1294-301; PMID:16410387; <http://dx.doi.org/10.1634/stemcells.2005-0342>.
- Qiao C, Xu W, Zhu W, Hu J, Qian H, Yin Q, et al. Human mesenchymal stem cells isolated from the umbilical cord. *Cell Biol Int* 2008; 32:8-15; PMID:17904875; <http://dx.doi.org/10.1016/j.cellbi.2007.08.002>.
- Wagner W, Wein F, Seckinger A, Frankhauser M, Wirkner U, Krause U, et al. Comparative characteristics of mesenchymal stem cells from human bone marrow, adipose tissue and umbilical cord blood. *Exp Hematol* 2005; 33:1402-16; PMID:16263424; <http://dx.doi.org/10.1016/j.exphem.2005.07.003>.
- Gondi CS, Veeravalli KK, Gorantla B, Dinh DH, Fassett D, Klopfenstein JD, et al. Human umbilical cord blood stem cells show PDGF-D-dependent glioma cell tropism in vitro and in vivo. *Neuro Oncol* 2010; 12:453-65; PMID:20406896.
- Kim DS, Kim JH, Lee JK, Choi SJ, Kim JS, Jeun SS, et al. Overexpression of CXCR4 chemokine receptors is required for the superior glioma-tracking property of umbilical cord blood-derived mesenchymal stem cells. *Stem Cells Dev* 2009; 18:511-9; PMID:18624673; <http://dx.doi.org/10.1089/scd.2008.0050>.
- Park SA, Ryu CH, Kim SM, Lim JY, Park SI, Jeong CH, et al. CXCR4-transfected human umbilical cord blood-derived mesenchymal stem cells exhibit enhanced migratory capacity toward gliomas. *Int J Oncol* 2011; 38:97-103; PMID:21109930.
- Dwyer RM, Potter-Beirne SM, Harrington KA, Lowery AJ, Hennessy E, Murphy JM, et al. Monocyte chemoattractant protein-1 secreted by primary breast tumors stimulates migration of mesenchymal stem cells. *Clin Cancer Res* 2007; 13:5020-7; PMID:17785552; <http://dx.doi.org/10.1158/1078-0432.CCR-07-0731>.
- Peled A, Petit I, Kollet O, Magid M, Ponomarev T, Byk T, et al. Dependence of human stem cell engraftment and repopulation of NOD/SCID mice on CXCR4. *Science* 1999; 283:845-8; PMID:9933168; <http://dx.doi.org/10.1126/science.283.5403.845>.
- Dasari VR, Velpula KK, Kaur K, Fassett D, Klopfenstein JD, Dinh DH, et al. Cord blood stem cell-mediated induction of apoptosis in glioma downregulates X-linked inhibitor of apoptosis protein (XIAP). *PLoS One* 2010; 5:11813; PMID:20676365; <http://dx.doi.org/10.1371/journal.pone.0011813>.
- Dasari VR, Kaur K, Velpula KK, Dinh DH, Tsung AJ, Mohanam S, et al. Downregulation of Focal Adhesion Kinase (FAK) by cord blood stem cells inhibits angiogenesis in glioblastoma. *Aging* 2010; 2:791-803; PMID:20228937.
- Dasari VR, Kaur K, Velpula KK, Gujrati M, Fassett D, Klopfenstein JD, et al. Upregulation of PTEN in glioma cells by cord blood mesenchymal stem cells inhibits migration via downregulation of the PI3K/Akt pathway. *PLoS One* 2010; 5:10350; PMID:20436671; <http://dx.doi.org/10.1371/journal.pone.0010350>.
- Gondi CS, Gogineni VR, Chetty C, Dasari VR, Gorantla B, Gujrati M, et al. Induction of apoptosis in glioma cells requires cell-to-cell contact with human umbilical cord blood stem cells. *Int J Oncol* 2010; 36:1165-73; PMID:20372790.
- Devine SM, Cobbs C, Jennings M, Bartholomew A, Hoffman R. Mesenchymal stem cells distribute to a wide range of tissues following systemic infusion into nonhuman primates. *Blood* 2003; 101:2999-3001; PMID:12480709; <http://dx.doi.org/10.1182/blood-2002-06-1830>.
- Oh W, Kim DS, Yang YS, Lee JK. Immunological properties of umbilical cord blood-derived mesenchymal stromal cells. *Cell Immunol* 2008; 251:116-23; PMID:18495100; <http://dx.doi.org/10.1016/j.cellimm.2008.04.003>.
- Cho PS, Messina DJ, Hirsh EL, Chi N, Goldman SN, Lo DP, et al. Immunogenicity of umbilical cord tissue derived cells. *Blood* 2008; 111:430-8; PMID:17909081; <http://dx.doi.org/10.1182/blood-2007-03-087774>.
- Ji F, Wang Y, Sun H, Du J, Zhao H, Wang D, et al. Human umbilical cord blood-derived non-hematopoietic stem cells suppress lymphocyte proliferation and CD4, CD8 expression. *J Neuroimmunol* 2008; 197:99-109; PMID:18534691; <http://dx.doi.org/10.1016/j.jneuroim.2008.04.013>.
- Wang M, Yang Y, Yang D, Luo F, Liang W, Guo S, et al. The immunomodulatory activity of human umbilical cord blood-derived mesenchymal stem cells in vitro. *Immunology* 2009; 126:220-32; PMID:18624725; <http://dx.doi.org/10.1111/j.1365-2567.2008.02891.x>.
- Yoo KH, Jang IK, Lee MW, Kim HE, Yang MS, Eom Y, et al. Comparison of immunomodulatory properties of mesenchymal stem cells derived from adult human tissues. *Cell Immunol* 2009; 259:150-6; PMID:19608159; <http://dx.doi.org/10.1016/j.cellimm.2009.06.010>.
- Velpula KK, Dasari VR, Tsung AJ, Dinh DH, Rao JS. Cord blood stem cells revert glioma stem cell EMT by downregulating transcriptional activation of Sox2 and Twist1. *Oncotarget* 2011; 2:1028-42; PMID:22184289.
- Velpula KK, Dasari VR, Tsung AJ, Gondi CS, Klopfenstein JD, Mohanam S, et al. Regulation of glioblastoma progression by cord blood stem cells is mediated by downregulation of cyclin D1. *PLoS One* 2011; 6:18017; PMID:21455311; <http://dx.doi.org/10.1371/journal.pone.0018017>.
- Jenhani F, Durand V, Ben Azoua N, Thallet S, Ben Othmen T, Bejaoui M, et al. Human cytokine expression profile in various conditioned media for in vitro expansion of bone marrow and umbilical cord blood immunophenotyped mesenchymal stem cells. *Transplant Proc* 2011; 43:639-43; PMID:21440783; <http://dx.doi.org/10.1016/j.transproceed.2011.01.021>.
- Liu CH, Hwang SM. Cytokine interactions in mesenchymal stem cells from cord blood. *Cytokine* 2005; 32:270-9; PMID:16377203; <http://dx.doi.org/10.1016/j.cyto.2005.11.003>.
- Ponte AL, Marais E, Gally N, Langonné A, Delorme B, Héralut O, et al. The in vitro migration capacity of human bone marrow mesenchymal stem cells: comparison of chemokine and growth factor chemotactic activities. *Stem Cells* 2007; 25:1737-45; PMID:17395768; <http://dx.doi.org/10.1634/stemcells.2007-0054>.
- Yan XL, Liu B, Mao N. Study on migration property of mesenchymal stem cells-review. *Zhongguo Shi Yan Xue Ye Xue Za Zhi* 2009; 17:1101-5; PMID:19698270.
- Peled A, Kollet O, Ponomarev T, Petit I, Franitza S, Grabovsky V, et al. The chemokine SDF-1 activates the integrins LFA-1, VLA-4 and VLA-5 on immature human CD34(+) cells: role in transendothelial/stromal migration and engraftment of NOD/SCID mice. *Blood* 2000; 95:3289-96; PMID:10828007.
- Bonavia R, Inda MM, Cavenee WK, Furnari FB. Heterogeneity maintenance in glioblastoma: a social network. *Cancer Res* 2011; 71:4055-60; PMID:21628493; <http://dx.doi.org/10.1158/0008-5472.CAN.11-0153>.

#### Acknowledgments

The authors thank Peggy Mankin and Noorjehan Ali for their technical assistance, Alicia Woodworth for manuscript preparation, Diana Meister and Sushma Jasti for manuscript review. The authors declare that no conflict of interest exists with this manuscript. Funding: This project was supported by award number NS057529 (to J.S.R.) from the National Institute of Neurological Disorders and Stroke (NINDS). Contents are solely the responsibility of the authors and do not necessarily represent the official views of NIH.



36. Lee J, Son MJ, Woolard K, Donin NM, Li A, Cheng CH, et al. Epigenetic-mediated dysfunction of the bone morphogenetic protein pathway inhibits differentiation of glioblastoma-initiating cells. *Cancer Cell* 2008; 13:69-80; PMID:18167341; <http://dx.doi.org/10.1016/j.ccr.2007.12.005>.
37. Vik-Mo EO, Sandberg C, Olstorn H, Varghese M, Brandal P, Ramm-Petersen J, et al. Brain tumor stem cells maintain overall phenotype and tumorigenicity after in vitro culturing in serum-free conditions. *Neuro Oncol* 2010; 12:1220-30; PMID:20843775.
38. Krause DS, Theise ND, Collector MI, Henegariu O, Hwang S, Gardner R, et al. Multi-organ, multi-lineage engraftment by a single bone marrow-derived stem cell. *Cell* 2001; 105:369-77; PMID:11348593; [http://dx.doi.org/10.1016/S0092-8674\(01\)00328-2](http://dx.doi.org/10.1016/S0092-8674(01)00328-2).
39. Tabatabai G, Bähr O, Möhle R, Eyüpoglu IY, Boehmler AM, Wischhusen J, et al. Lessons from the bone marrow: how malignant glioma cells attract adult haematopoietic progenitor cells. *Brain* 2005; 128:2200-11; PMID:15947066; <http://dx.doi.org/10.1093/brain/awh563>.
40. Schmidt NO, Przylecki W, Yang W, Ziu M, Teng Y, Kim SU, et al. Brain tumor tropism of transplanted human neural stem cells is induced by vascular endothelial growth factor. *Neoplasia* 2005; 7:623-9; PMID:16036113; <http://dx.doi.org/10.1593/neo.04781>.
41. Kim SM, Lim JY, Park SI, Jeong CH, Oh JH, Jeong M, et al. Gene therapy using TRAIL-secreting human umbilical cord blood-derived mesenchymal stem cells against intracranial glioma. *Cancer Res* 2008; 68:9614-23; PMID:19047138; <http://dx.doi.org/10.1158/0008-5472.CAN-08-0451>.
42. Ryu CH, Park SH, Park SA, Kim SM, Lim JY, Jeong CH, et al. Gene therapy of intracranial glioma using interleukin 12-secreting human umbilical cord blood-derived mesenchymal stem cells. *Hum Gene Ther* 2011; 22:733-43; PMID:21261460; <http://dx.doi.org/10.1089/hum.2010.187>.
43. Park JH, Ryu JM, Han HJ. Involvement of caveolin-1 in fibronectin-induced mouse embryonic stem cell proliferation: role of FAK, RhoA, PI3K/Akt and ERK 1/2 pathways. *J Cell Physiol* 2011; 226:267-75; PMID:20658539; <http://dx.doi.org/10.1002/jcp.22338>.
44. Chen J, Li Y, Wang L, Zhang Z, Lu D, Lu M, et al. Therapeutic benefit of intravenous administration of bone marrow stromal cells after cerebral ischemia in rats. *Stroke* 2001; 32:1005-11; PMID:11283404; <http://dx.doi.org/10.1161/01.STR.32.4.1005>.
45. Wang L, Li Y, Chen J, Gautam SC, Zhang Z, Lu M, et al. Ischemic cerebral tissue and MCP-1 enhance rat bone marrow stromal cell migration in interface culture. *Exp Hematol* 2002; 30:831-6; PMID:12135683; [http://dx.doi.org/10.1016/S0301-472X\(02\)00829-9](http://dx.doi.org/10.1016/S0301-472X(02)00829-9).
46. Wang L, Li Y, Chen X, Chen J, Gautam SC, Xu Y, et al. MCP-1, MIP-1, IL-8 and ischemic cerebral tissue enhance human bone marrow stromal cell migration in interface culture. *Hematology* 2002; 7:113-7; PMID:12186702; <http://dx.doi.org/10.1080/10245330290028588>.
47. Ji JF, He BP, Dheen ST, Tay SS. Interactions of chemokines and chemokine receptors mediate the migration of mesenchymal stem cells to the impaired site in the brain after hypoglossal nerve injury. *Stem Cells* 2004; 22:415-27; PMID:15153618; <http://dx.doi.org/10.1634/stemcells.22-3-415>.
48. Bieback K, Kern S, Klüter H, Eichler H. Critical parameters for the isolation of mesenchymal stem cells from umbilical cord blood. *Stem Cells* 2004; 22:625-34; PMID:15277708; <http://dx.doi.org/10.1634/stemcells.22-4-625>.
49. von Drygalski A, Adamson JW. Placental/umbilical cord blood (PCB) stem cells for transplantation: early clinical outcomes and the status of ex vivo expansion strategies. *Keio J Med* 2000; 49:141-51; PMID:11192982; <http://dx.doi.org/10.2302/kjm.49.141>.
50. Weiss ML, Mitchell KE, Hix JE, Medicetty S, El-Zarkouny SZ, Grieger D, et al. Transplantation of porcine umbilical cord matrix cells into the rat brain. *Exp Neurol* 2003; 182:288-99; PMID:12895440; [http://dx.doi.org/10.1016/S0014-4886\(03\)00128-6](http://dx.doi.org/10.1016/S0014-4886(03)00128-6).
51. Uccelli A, Pistoia V, Moretta L. Mesenchymal stem cells: a new strategy for immunosuppression? *Trends Immunol* 2007; 28:219-26; PMID:17400510; <http://dx.doi.org/10.1016/j.it.2007.03.001>.
52. Lee J, Kotliarova S, Kotliarov Y, Li A, Su Q, Donin NM, et al. Tumor stem cells derived from glioblastomas cultured in bFGF and EGF more closely mirror the phenotype and genotype of primary tumors than do serum-cultured cell lines. *Cancer Cell* 2006; 9:391-403; PMID:16697959; <http://dx.doi.org/10.1016/j.ccr.2006.03.030>.
53. Lakka SS, Gondi CS, Yanamandra N, Olivero WC, Dinh DH, Gujrati M, et al. Inhibition of cathepsin B and MMP-9 gene expression in glioblastoma cell line via RNA interference reduces tumor cell invasion, tumor growth and angiogenesis. *Oncogene* 2004; 23:4681-9; PMID:15122332; <http://dx.doi.org/10.1038/sj.onc.1207616>.